Proc. Natl. Acad. Sci. USA
Vol. 89, pp. 314–318, January 1992
Medical Sciences

Ongoing enterovirus-induced myocarditis is associated with persistent heart muscle infection: Quantitative analysis of virus replication, tissue damage, and inflammation

(coxsackievirus B3/picornavirus/*in situ* hybridization/mouse model/digital image analysis)

KARIN KLINGEL*, CHRISTINE HOHENADL*, ANNIE CANU†, MICHAELA ALBRECHT*, MARKUS SEEMANN‡, GERHARD MALL‡, AND REINHARD KANDOLF*§

*Max-Planck-Institut für Biochemie, D-8033 Martinsried, Federal Republic of Germany; †Départément de Microbiologie, Unité de Formation et de Recherche des Sciences Pharmaceutiques, F-14000 Caen, France; ‡Pathologisches Institut, Universität Heidelberg, D-6900 Heidelberg, Federal Republic of Germany; and §Medizinische Klinik I, Universität München, D-8000 München, Federal Republic of Germany

Communicated by Charles Weissmann, September 24, 1991 (received for review June 4, 1991)

ABSTRACT **Coxsackievirus B3-induced myocarditis in different immunocompetent mouse strains was used as a model to investigate interrelationships between virus replication and development of chronic enteroviral heart disease. Using *in situ* hybridization to detect enteroviral RNA, we show that heart muscle infection is not only detected in acute myocarditis but is also detected during the chronic phase of the disease. Coxsackievirus B3 could evade immunological surveillance in a host-dependent fashion, thus inducing a persistent infection of the myocardium in association with ongoing inflammation. Patterns of acute and persistent myocardial infection were quantitatively assessed in one representative mouse strain (A.CA/SnJ, H-2^f) by applying computer-assisted digital image processing; these patterns were then related to the extent of myocardial tissue damage as well as to inflammation. We observed a strong correlation, both spatial and temporal, between viral replication and development of myocardial lesions, indicating that acute and chronic myocardial injuries are a consequence of multifocal organ infection. Analysis of strand-specific *in situ* hybridization revealed that viral replication in persistent infection is restricted at the level of RNA synthesis. The described procedure for quantitating organ infection provides a powerful tool for evaluating virus–host interactions and will be of particular interest to those studying human enterovirus-induced cardiomyopathies.**

Enteroviruses of the human Picornaviridae, such as the group B coxsackieviruses (types 1–5), are known to be important etiologic agents of viral myocarditis (1–3). Other members of the enterovirus group, comprising at present ≈70 distinct serotypes (e.g., various group A viruses and echoviruses), have also been associated with human viral heart disease. These RNA viruses, which contain a single-stranded RNA genome of positive polarity, can induce dilated cardiomyopathy of acute onset or lead to life-threatening arrhythmias and sudden death.

Regarding the pathogenesis of this heart disease, a controversy exists as to whether myocardial injury results from virus-induced pathobiological events or from autoimmune processes initially triggered by viral infection of the heart (4). If viral products are required for the development and sustainment of myocardial lesions, a strong correlation between viral replication and tissue injury should exist. On the other hand, if autoimmune mechanisms are crucial for lesion formation, heart tissue damage should evolve independently of virus replication. To study enterovirus replication in heart tissue at the cellular level we previously developed an *in situ* hybridization technique using recombinant coxsackievirus B3 (CVB3) cDNA as an enterovirus-specific probe (5, 6). With this technique, enterovirus RNA could not only be detected in myocardial biopsy samples of patients with acute and chronic myocarditis but also in patients with end-stage dilated cardiomyopathy, indicating that chronic myocardial injury may be associated with persistent enterovirus infection (3).

We now report on persistent myocardial enterovirus infection in various immunocompetent mouse strains. Based on an interactive digital image analysis system, patterns of myocardial infection were quantitatively correlated with the extent of myocardial injury and cellular immune response. Here we show that CVB3, typically a cytolytic virus, can induce a persistent infection *in vivo*. In this study we further demonstrate that a relatively small number of infected cells is sufficient for the maintenance of tissue lesions and inflammation as observed during the chronic phase of the disease. The importance of viral replication in the pathogenesis of ongoing heart muscle disease is substantiated by the finding that tissue lesions, as well as inflammatory cells, did not evolve independently of virus replication.

MATERIAL AND METHODS

Virus, Cells, and Animals. Transfection-derived CVB3 (Nancy strain) (5) was passaged three times in murine hearts to increase its myocarditic potential and further propagated on Vero cells. Four-week-old male immunocompetent inbred mice [strains A.CA/SnJ (H-2^f), A.BY/SnJ (H-2^b), SWR/J (H-2^q), and DBA/1J (H-2^q), The Jackson Laboratory] were inoculated i.p. with 6×10^4 plaque-forming units of CVB3. Twenty-eight animals of each strain were sacrificed at days 6, 12, 18, and 30 postinfection (p.i.). For quantitative investigations, in addition, 100 A.CA/SnJ mice were sacrificed at days 3, 6, 9, 12, 15, 18, 24, and 30 p.i. Eighty-four percent of the infected A.CA/SnJ mice developed myocardial lesions in the presence of infectious CVB3 as seen by routine virus reisolation up to 15 days p.i. Twenty-four percent of the A.CA/SnJ mice died between day 6 and 11 p.i. None of the 24 mock-infected control mice died spontaneously.

Processing of Myocardial Tissue. Aseptically removed hearts were transversely dissected, and tissue samples were either quick-frozen in liquid nitrogen or fixed for 2 hr at 4°C by immersion in 1.5% paraformaldehyde/1.5% glutardialdehyde/0.1 M sodium phosphate buffer, pH 7.2 and embedded in paraffin. For *in situ* hybridization, serial sections (4 μm) were mounted on microscopic slides that had been cleaned in

The publication costs of this article were defrayed in part by page charge payment. This article must therefore be hereby marked "*advertisement*" in accordance with 18 U.S.C. §1734 solely to indicate this fact.

Abbreviations: CVB3, coxsackievirus B3; p.i., postinfection.

10% Extran MA 01 (Merck) and coated with 3-aminopropyl-3-ethoxysilane.

Preparation of Labeled DNA and RNA Probes. Recombinant CVB3 cDNA (5) containing a full-length transcript of the viral genome was digested with *Kpn* I or *Bam*HI restriction endonuclease to generate a virus-specific 6.2-kilobase (kb) and 1.0-kb fragment, respectively, corresponding to nucleotides 66–7128 of the viral genome (7). CVB3 cDNA fragments were purified twice by agarose gel electrophoresis and radiolabeled by nick-translation using deoxyadenosine [α-[^{35}S]thio]triphosphate and deoxycytidine [α-[^{35}S]thio] triphosphate (1200 Ci/mmol; 1 Ci = 37 GBq) as described (6). The specific activity was 3–5 × 10^8 dpm/μg of DNA. Control DNA probes were prepared from nonrecombinant plasmid vector p2732B (5).

Single-stranded ^{35}S-labeled RNA probes for strand-specific detection of viral plus- or minus-strand RNA were synthesized from the dual-promoter plasmid pCVB3-R1 by using either T7 or SP6 RNA polymerase (8). Control RNA probes were synthesized from nonrecombinant transcription vector pSPT18.

***In Situ* Hybridization.** Dewaxed paraffin heart tissue sections were hybridized basically as described (6). Hybridization mixture contained either the ^{35}S-labeled CVB3 cDNA probe (200 ng/ml) or CVB3 strand-specific RNA probes (500 ng/ml) in 10 mM Tris·HCl, pH 7.4/50% (vol/vol) deionized formamide/600 mM NaCl/1 mM EDTA/0.02% polyvinylpyrrolidone/0.02% Ficoll/0.05% bovine serum albumin/10% dextran sulfate/10 mM dithiothreitol/denatured sonicated salmon sperm DNA at 200 μg/ml/rabbit liver tRNA at 100 μg/ml. Hybridization with DNA probes proceeded at 25°C for 36 hr, whereas hybridization with RNA probes was done at 42°C for 18 hr. Slides were then washed as described (6) followed by 1 hr at 55°C in 2× standard saline citrate. Nonhybridized single-stranded RNA probes were digested by RNase A (20 μg/ml) in 10 mM Tris·HCl, pH 8.0/0.5 M NaCl for 30 min at 37°C (8). Myocardial slide preparations were autoradiographed as described (6) and stained with hematoxylin/eosin.

Immunohistochemistry. For characterization of inflammatory cells, cryostat heart tissue sections (4 μm) were incubated for 1 hr at 25°C with a panel of rat anti-mouse monoclonal antibodies recognizing (*i*) Mac$^+$ (macrophages, clone M1/70 HL, Boehringer Mannheim), (*ii*) Lyt2$^+$ (cytotoxic/suppressor T lymphocytes, clone YTS 169.4, Sera-Lab Crawley Down, Sussex, U.K.), (*iii*) L3T4$^+$ (helper T cells, clone YTS 191.1, Sera-Lab) positive cells followed by visualization with a biotin–streptavidin–immunoperoxidase technique (9). Controls using normal rat serum were done to exclude nonspecific staining.

Quantification of *In Situ* Hybridization. Myocardial *in situ* autoradiographs were processed by means of the automatic image analyzing system IBAS II (Kontron, Zürich). Myocardial slide preparations were examined with a Leitz microscope and a black-and-white video camera at a primary magnification of ×40; the video signals were transformed to a digital format under interactive visual control. *In situ* hybridization-positive cells were segmented from background grains by applying a chain-code algorithm as described (10). Area fractions of infected myocardial tissue [A_A infection—area of hybridization-positive myocardium per total area of myocardium ($\mu m^2/mm^2$)] were computed on transverse tissue sections of the whole heart, including the left and right ventricle.

Morphometric Analysis of Myocardial Tissue Damage. The extent of myocardial lesions was quantified on hematoxylin/eosin-stained transverse sections of the heart chambers. Myocardial damage was defined as myocardial cell necrosis, inflammation, or scarring. Thirty visual fields per heart were selected by systematic random sampling, and myocardial tissue lesions were quantified at a primary magnification of ×160. The area fraction of damaged myocardium [A_A damage—area of damage per total area of myocardium ($\mu m^2/mm^2$)] was calculated with point counting, according to standard morphometric procedures (11).

Statistical Evaluation of Quantitative Data. One-way analysis of variance and Scheffe's test were used to detect significant differences at indicated time points. P values <0.05 were considered statistically significant.

RESULTS

Patterns of Acute and Persistent Myocardial Organ Infection. To investigate the natural course of myocardial enterovirus infection in immunocompetent mice, the presence of CVB3 RNA was followed systematically by *in situ* hybridization in different mouse strains (A.CA/SnJ, A.BY/SnJ, SWR/J, and DBA/1J). As histopathologic changes were comparable in mouse strains revealing persistent infection, the myocardial infection pattern, as well as all quantitative investigations, is described for the representative mouse strain A.CA/SnJ. Two to 3 days p.i. individual *in situ*-positive myocytes were found randomly distributed throughout the right and left ventricle of the heart, indicating hematogenous infection of myocytes during viremia (Fig. 1*A*). The high local autoradiographic grain densities in hybridization-positive cells demonstrate high-copy numbers of replicating viral genomes in acutely infected myocytes. The typical *in situ* pattern of acute heart muscle injury 6 days p.i. is illustrated in Fig. 1*B*. Infected myocytes are observed adjacent to foci of inflammation, which provide the basis for the histopathologic diagnosis of acute myocarditis.

In the acute stage of the disease most infected cells were found associated with multifocal lesions, but clusters of infected myocytes were also seen in areas of noninflamed myocardial tissue (Fig. 1*B*), indicating that direct cell-to-cell spread of the virus is involved in the pathogenesis of ongoing myocardial infection. Transverse sections of the myocardium (Fig. 1*C*) revealed a transmural and multifocal infection of the heart with involvement of both ventricle walls, including the interventricular septum and also epicardial and endocardial muscle layers. Between day 12 and 15 p.i., when maximum cellular infiltration was noted, the number of infected myocardial cells decreased (Fig. 1*D*). Nonetheless, whenever myocardial lesions were observed at later disease stages, they were consistently associated with infected myocardial cells. Persistently infected myocardial cells were found primarily located within foci of chronic myocardial lesions containing replacement fibrosis, degenerated myocytes, and mononuclear cell infiltrates.

Fig. 1*E* represents the typical *in situ* pattern of persistent myocardial CVB3 infection 30 days p.i.; this pattern is characterized by ongoing inflammation in the presence of infected myocardial cells, which exhibited a decreased copy number of viral RNA (as reflected by the decreased autoradiographic grain densities) when compared with acute infection. Viral persistence in association with ongoing inflammatory lesions was also seen in the hearts of inbred mouse strains A.BY/SnJ and SWR/J. In contrast, DBA/1J mice were found able to clear the virus during acute disease; no ongoing myocardial inflammation was noted in this mouse strain after day 18 p.i.

Quantitative Evaluation of Myocardial Infection. Fig. 2 illustrates an example of computerized automatic image analysis adapted for quantitative analysis of myocardial *in situ* hybridization in this study. Autoradiographic signals (Fig. 2*A*) were measured under visual control by application of a grey-value threshold corresponding to 90 grains per infected myocyte (local grain density of *in situ* hybridization-positive cells was ≥ 0.3 per μm^2). Uninfected myocytes

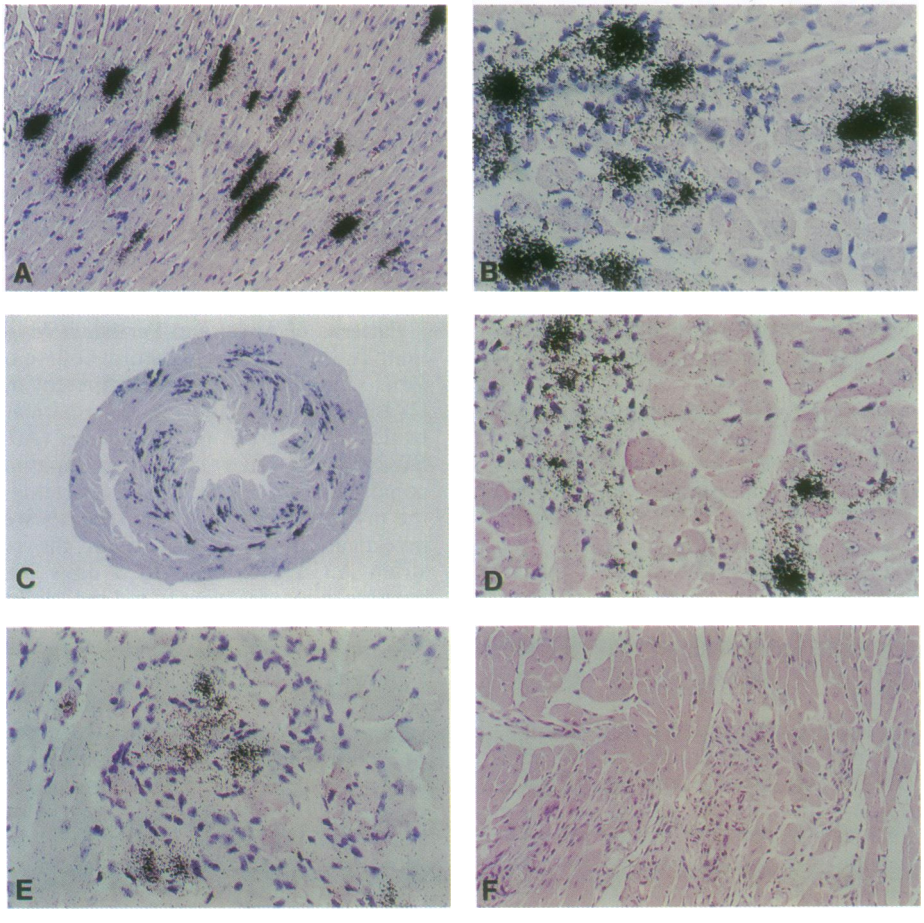

FIG. 1. *In situ* detection of CVB3 RNA in murine myocardial tissue during enteroviral infection. Paraffin-embedded heart tissue sections (4 μm) obtained 3 days (*A*), 6 days (*B* and *C*), 12 days (*D*), or 30 days (*E*) after i.p. CVB3 infection of A.CA/SnJ mice were hybridized with the ^{35}S-labeled CVB3 cDNA probe and exposed for 2 weeks. No labeling of infected myocardial cells was seen when myocardial tissue sections were hybridized with ^{35}S-labeled plasmid vector p2732B control DNA (*F*, 30 days p.i.). [Hematoxylin/eosin; (*A* and *F*) ×100, (*B*) ×255, (*C*) ×10, (*D* and *E*) ×200.]

consistently revealed <20 grains (grain density of background was <0.07 per μm^2). Thus, positivity and negativity of hybridized cells were defined as a binary variable. After digital processing of *in situ* hybridization (Fig. 2*B*), the areas, as well as the diameters (D_{max}, D_{min}), of infected cells were measured automatically. Areas of hybridization-positive heart muscle cells were referred to the total area of the tissue section and expressed in area percent or as area fraction of infection in $\mu m^2/mm^2$. Reproducibility of this image analysis procedure was confirmed by an interobserver coefficient of variation of <3%.

Quantitative Characterization of Acute and Persistent Myocardial Infection. The morphometrical quantification of myocardial infection after digital image processing (Fig. 3*A*) revealed increased area fractions of infected cardiac tissue until day 9 after CVB3 infection, when up to 13% of the myocardial cells was infected. Thereafter, decreased area fractions of infected myocardial tissue were found, reflecting a significantly reduced number of infected myocardial cells at later stages of the disease compared with the acute infection ($P < 0.001$). During persistent infection—e.g., 30 days p.i.—≈0.01% of myocardial cells were found to be infected.

Corresponding to the *in situ* hybridization results, the maximum of myocardial tissue damage (consisting of virus-induced myocytolysis, inflammation, and scarring) was detected during the acute infection (Fig. 3*A*). A histomorphometrically significant increase in myocardial injury was measured during acute myocarditis (day 6 and 9 p.i., $P < 0.001$) but was not seen at later disease stages (days 12–30 p.i.).

Concurrent with increased area fractions of infected myocardial tissue, an increase in numerical densities of macrophages and T lymphocytes was observed during acute infection (Fig. 3*B*). In early infection (up to day 6 p.i.), the number of cytotoxic/suppressor T lymphocytes (Lyt2$^+$) exceeded the number of T helper cells (L3T4$^+$). The maximum densities of mononuclear infiltrates was reached 12 days p.i. and coincides with the beginning decrease in area fractions of *in situ*-positive cells, indicating that macrophages and T lymphocytes are crucial in limiting virus dissemination in the heart. Despite this prominent cell-mediated immune response (Fig. 3*B*), the virus was found capable of evading immunologic surveillance and inducing a persistent infection (Fig. 1*E*).

Strand-Specific Detection of Viral Plus- and Minus-Strand RNA. The reduced number of infected cells, in addition to decreased copy numbers of viral genomes during persistent infection, (compare Fig. 1*D* and *E*) suggests that virus replication is restricted during ongoing myocarditis. To characterize restricted replication at the level of viral RNA synthesis, single-stranded RNA probes that allow differential detection of plus- and minus-strand RNA were used for *in situ* hybridization (Fig. 4). Both forms of viral RNA, genomic plus-strand RNA as well as the intermediate minus-strand RNA, were detected in the same myocardial cells, as visualized on serial tissue sections. The acute myocardial infection was characterized by a striking difference in autoradiographic silver grain densities between viral plus-strand RNA (Fig. 4*A*) and viral minus-strand RNA (Fig. 4*B*). During acute infection, viral genomic plus-strand RNA is synthesized in

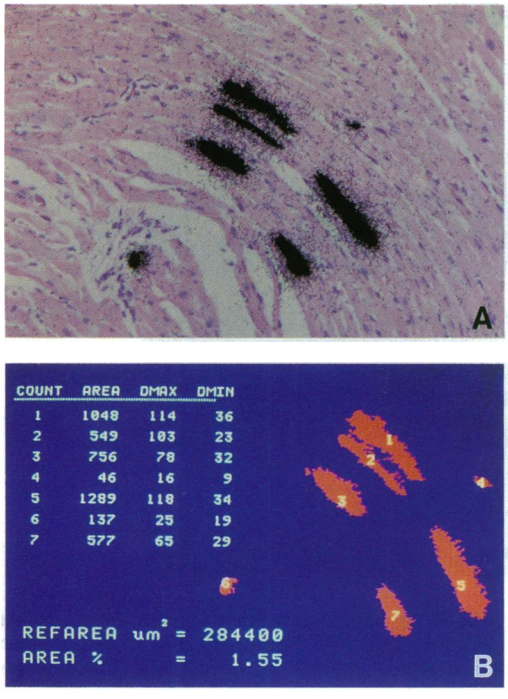

FIG. 2. Quantitative image analysis of *in situ* hybridization. (*A*) Original image showing CVB3 RNA visualized by autoradiography after *in situ* hybridization. (×115.) (*B*) Corresponding image after digital processing. The digital image consisted of 512 × 512 pixels with a grey-value range of 0–255 for each pixel. The interactive computer image analysis system allows measurement of areas and diameters (D_{max}, D_{min}) of autoradiographic signals.

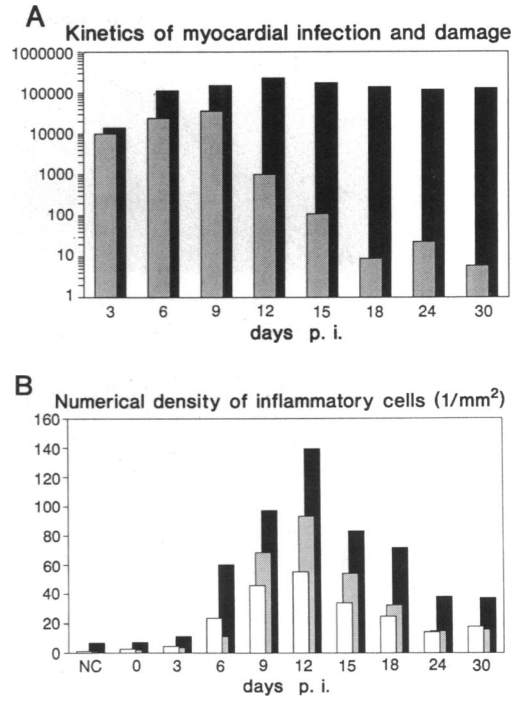

FIG. 3. Quantitative characterization of myocardial CVB3 infection in A.CA/SnJ mice. (*A*) Kinetics of area fractions of *in situ* hybridization-positive heart tissue (A_A infection, ▩) and area fractions of myocardial tissue damage (A_A damage, ■). (*B*) Cellular immune response during infection: Macl$^+$ (macrophages) (■), Lyt2$^+$ (cytotoxic/suppressor T lymphocytes) (□), and L3T4$^+$ (helper T lymphocytes) (▩). Quantification of immunohistochemically positive cells was achieved by counting at a magnification of ×400 in 150 randomly selected quadrats (mean area was 50,000 μm^2) per tissue section. Results are expressed as arithmetic means of 7–12 animals per time point.

great excess in comparison with the synthesis of relatively low-copy numbers of the minus-strand RNA intermediate. In contrast to acute infection, the amount of viral plus-strand RNA (Fig. 4*C*) in myocardial cells of persistently infected mice appears similar to the amount of minus-strand RNA (Fig. 4*D*). These results demonstrate that viral replication in persistent enterovirus infection is restricted at the level of viral RNA synthesis.

Moreover, viral capsid protein expression was studied by immunohistochemistry with polyclonal antisera that have been raised against two nonoverlapping bacterially synthesized structural fusion proteins of CVB3 (12). The results indicate that the amount of enteroviral capsid protein synthesis is decreased in persistently infected cells (data not shown), thus reflecting restricted viral RNA replication.

DISCUSSION

Recent *in situ* hybridization studies in patients provided evidence that enterovirus infection is detectable in all stages of acute and chronic myocarditis, as well as in end-stage dilated cardiomyopathy, suggesting the possibility of enterovirus persistence in the human heart (3). Experimentally, acute and chronic enterovirus-induced myocarditis has been described in various murine models (13), which exhibit histopathologic findings resembling heart muscle lesions seen in humans.

In this investigation we have followed the natural course of CVB3-induced myocarditis in genetically different immunocompetent mouse strains using *in situ* hybridization to detect viral RNA. Importantly, we found that CVB3 can induce a persistent infection in A.CA/SnJ (H-2^f), A.BY/SnJ (H-2^b), and SWR/J (H-2^q) mice but cannot induce persistent infection in DBA/1J (H-2^q) mice, indicating that host genetics are a major determinant of chronic myocardial disease. A strong correlation, both spatial and temporal, between viral replication and formation of lesions was not seen only during acute myocardial infection but was seen also during chronic disease. No inflammatory lesions were found to evolve in the absence of virus replication during the disease. Our finding in DBA/1J mice that inflammatory myocardial processes can be terminated by eliminating the virus from the heart implies that the development of chronic disease depends on viral persistence. In addition, our previous observations of ongoing severe myocardial tissue lesions in persistently CVB3-infected T-cell-deficient NMRI (*nu/nu*) mice (6) support the concept that myocardial injury is the consequence of virus-induced cytopathology. Thus, from our results it can be concluded that immune-mediated processes described for chronic enterovirus-induced myocarditis (4) are triggered by persistent infection.

The early infiltration of macrophages and T lymphocytes is the characteristic histological hallmark of viral myocarditis (14). During acute infection, cytotoxic T lymphocytes identify and destroy infected myocytes, expressing major histocompatibility complex class I molecules (15). The progression of acute infection, according to our results, is characterized by a rapid exacerbation of myocardial lesions (up to day 12 p.i.) and increases in the area fractions of infected myocardial cells (up to day 9 p.i.) and in inflammatory cell densities (up to day 12 p.i.). From the mean volume of myocytes (12,000 μm^3), the area fraction of myocytes (85% of heart cells) and the area fraction of *in situ* hybridization-positive cells, it can be estimated—according to basic stereological principles (11)—that 1 mm^3 of myocardial tissue contains, on average, 3000 infected myocytes on day 9 p.i. However, morphometrical evaluation of myocardial damage suggests myocytolysis and necrosis of ≈11,000 myocytes per

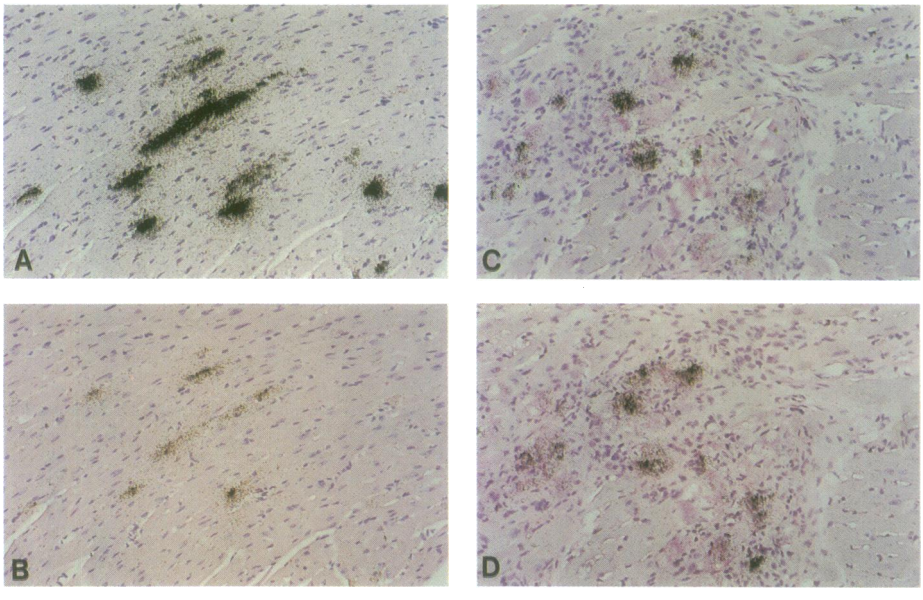

FIG. 4. Strand-specific detection of CVB3 plus- and minus-strand RNA after 3 weeks of autoradiographic exposure. *In situ* hybridization of serial sections from acutely infected myocardium (*A* and *B*) revealed that viral plus-strand RNA (*A*) appears in great excess compared with minus-strand RNA (*B*), whereas in persistently infected hearts (*C* and *D*) the amount of viral plus-strand RNA (*C*) resembles that of minus-strand RNA (*D*). (×100.)

mm^3 of myocardium at that time point. This observation can be explained by a relatively short mean-time survival of acutely infected myocytes. Provided that the expansion of myocardial injury between day 3 and 9 p.i. can be described by an exponential function, infected myocytes survive ≈24 h during acute replication. This figure agrees with earlier observations in CVB3-infected cultured myocytes (16).

In the present study we showed that ongoing enterovirus-induced myocarditis is based on persistent infection. Quantitative analysis of *in situ* hybridization indicated that during chronic disease up to 30 cardiac cells are infected in 1 mm^3 of heart tissue, which is obviously sufficient to sustain myocardial inflammation. In addition, we found that virus persistence in the heart is associated with restricted viral RNA and capsid protein synthesis. Altered replication and transcription of virus, in addition to an immune response insufficient to recognize and clear virus-infected cells entirely, are essential mechanisms for the initiation and maintenance of a persistent infection (17). Restricted replication may also explain the failure to reisolate infectious virus after day 15 p.i., which, however, does not exclude the presence of very low infectivity titers.

The observation of restricted viral replication described in this study appears similar to that reported on Theiler virus infection, a murine picornavirus responsible for a persistent demyelinating infection of the central nervous system. In this type of persistent infection, the amount of inflammation paralleled the virus replication, which was restricted at the level of RNA transcription and capsid antigen synthesis (18, 19).

Besides the strategy of restricted replication, viruses are known to establish persistence by infection of cellular constituents of the immune system itself (20). Preliminary observations in CVB3-infected mice revealed that during the chronic phase of the disease, in addition to heart muscle cells, spleen and lymph nodes exhibited persistent infection of lymphoid cells, which might play a role in dissemination of virus or maintenance of a noncardiac viral reservoir.

The availability of the described murine model of persistent CVB3 heart muscle infection should prove useful for further studies on viral and immunological mechanisms of enterovirus-induced cardiomyopathy—e.g., with regard to identification of host genes involved in the development of chronic disease.

We thank Dr. P. H. Hofschneider for helpful discussions and critical reading of the manuscript. The excellent technical assistance of P. Rieger and H. Riesemann is appreciated. This work was supported, in part, by Grants Ka 593/2-2 and Kl 595/1-1 from the Deutsche Forschungsgemeinschaft and by Grant 321-7291-BCT-0370 "Grundlagen und Anwendungen der Gentechnologie" from the German Ministry for Research and Technology. R.K. is a Hermann and Lilly Schilling Professor of Medical Research.

1. Abelmann, W. H. (1973) *Annu. Rev. Med.* **24,** 145–152.
2. Melnick, J. L. (1990) in *Virology*, eds. Fields, B. N. & Knipe, D. M. (Raven, New York), Vol. 1, pp. 549–605.
3. Kandolf, R. & Hofschneider, P. H. (1989) *Springer Semin. Immunopathol.* **11,** 1–13.
4. Leslie, K., Blay, R., Haisch, C., Lodge, A., Weller, A. & Huber, S. (1989) *Clin. Microbiol. Rev.* **2,** 191–203.
5. Kandolf, R. & Hofschneider, P. H. (1985) *Proc. Natl. Acad. Sci. USA* **82,** 4818–4822.
6. Kandolf, R., Ameis, D., Kirschner, P., Canu, A. & Hofschneider, P. H. (1987) *Proc. Natl. Acad. Sci. USA* **84,** 6272–6276.
7. Klump, W. M., Bergmann, I., Müller, B. C., Ameis, D. & Kandolf, R. (1990) *J. Virol.* **64,** 1573–1583.
8. Hohenadl, C., Klingel, K., Mertsching, J., Hofschneider, P. H. & Kandolf, R. (1991) *Mol. Cell. Probes* **5,** 11–20.
9. Rovin, B. H., Harris, K. P. G., Morrison, A., Klahr, S. & Schreiner, G. F. (1990) *Lab. Invest.* **63,** 213–220.
10. Freeman, H. (1970) in *Picture Processing and Psychopictories*, eds. Lipkin, B. S. & Rosenfeld, A. (Academic, New York), pp. 241–266.
11. Weibel, E. R. (1979) *Stereological Methods* (Academic, New York).
12. Werner, S., Klump, W. M., Schönke, H., Hofschneider, P. H. & Kandolf, R. (1988) *DNA* **7,** 307–316.
13. Herskowitz, A., Wolfgram, L. J., Rose, N. R. & Beisel, K. W. (1987) *J. Am. Coll. Cardiol.* **57,** 1311–1319.
14. Godeny, E. K. & Gauntt, C. J. (1987) *Am. J. Pathol.* **129,** 267–276.
15. Seko, Y., Tsuchimochi, H., Nakamura, T., Okumura, K., Naito, S., Imataka, K., Fujii, J., Takaku, F. & Yazaki, Y. (1990) *Circ. Res.* **67,** 360–367.
16. Kandolf, R., Canu, A. & Hofschneider, P. H. (1985) *J. Mol. Cell. Cardiol.* **17,** 167–181.
17. Oldstone, M. B. A. (1989) *Cell* **56,** 517–520.
18. Chamorro, M., Aubert, C. & Brahic, M. (1986) *J. Virol.* **57,** 992–997.
19. Cash, E., Chamorro, M. & Brahic, M. (1988) *J. Virol.* **62,** 1824–1826.
20. Pomeroy, C., Hilleren, P. J. & Jordan, M. C. (1991) *J. Virol.* **65,** 3330–3334.